2011 IEEE/RSJ International Conference on
Intelligent Robots and Systems
September 25-30, 2011. San Francisco, CA, USA

Synthesis of a Non-Circular Cable Spool to Realize a Nonlinear Rotational Spring

Nicolas Schmit and Masafumi Okada

Abstract— **In this paper we present a cable mechanism which realizes a nonlinear rotational spring from a linear translational spring. The spring is pulled by a cable wound around a non-circular spool, which is rigidly attached to the joint. The non-circular shape of the spool induces a nonlinear relationship between its angular position and the torque created by the tension of the cable. Depending on the shape of the spool, various torque profiles can be realized. We show that for a given nonlinear torque profile, there is a closed-form solution of the shape of the spool which synthesizes this function. In a first part, we present the geometry of the problem. In a second part, we derive the methodology to calculate the shape of the spool to synthesize a prescribed torque profile. In the last part, we verify the design methodology by experiments with three different spools realizing a constant force spring, an exponential softening spring and a cubic polynomial spring. We discuss the possible sources of errors between the theoretical and experimental results.**

I. INTRODUCTION

Robotic devices used for industrial process are generally designed with very stiff links and joints to ensure an accurate and high speed positioning of the end-effector. However, in the growing field of wearable robotics, rehabilitation robotics, prosthetics, and walking robots, the implementation of softness in robotic joints has become mandatory to match the requirements of shock absorption, smooth interaction with the user, and energy saving. Furthermore, when designing a compliant joint as the solution of an optimization problem, we could improve the performances of the system if we do not restrain to linear stiffness. This is because a nonlinear load-displacement function offers more design parameters than a linear function, and because the space of linear functions is a subspace of the space of continuous functions.

Various applications, including (but not limited to) robotics, can benefit from nonlinear stiffness. In shock absorption devices, a hardening spring can reduce the stopping distance while a softening spring can be advisable when the structural element to be protected is unable to withstand high accelerations [1]. In manipulators, a nonlinear spring mechanism can be implemented so that the stiffness of the link drops abruptly if the external force exceeds a critical force, thus guaranteeing the collision safety [2, 3]. In vibration damping, nonlinear springs can be used to create a Nonlinear Energy Sink (NES) capable of absorbing steady state vibration energy from the main system over a relatively broad frequency range [4, 5]. Nonlinear stiffness also plays a crucial role in running/hopping robots [6]. It can improve the energy efficiency [7], and the stability [8] of the motion. Finally, it is worth noticing several attempts to design simultaneously the control law and the mechanism of controlled multibody systems as the solution of an optimization problem [9, 10]. Although the methods presented in these last two papers consider only linear stiffness, we could imagine an extension to the design of nonlinear stiffness.

The implementation of nonlinear stiffness in a robotic device can be mainly achieved by two ways. The first one is to design a compliant element with a nonlinear load-displacement function (nonlinear spring) [11, 12, 13, 14]. The second method is to connect a linear spring to a nonlinear transmission mechanism. This method has the benefit of using an off-the-shelf linear spring, but the drawback of the weight and size of the transmission mechanism. The design of the transmission mechanism can be achieved by optimizing the design parameters (length of links, etc.) of the mechanism to minimize the error between the prescribed and achieved load-displacement function [15]. A more accurate but complicated strategy consists in a direct computation of a part of the mechanism to synthesize exactly the prescribed load-displacement function. The nonlinearity can result from rollers moving on a curved surface [16, 17], cams [18, 19] or from a varying radius shaft placed inside of a torsion spring [20]. Some authors also proposed a mechanism where the compliant element is replaced by torque-controlled actuators [21].

In this paper we present a cable mechanism which realizes a nonlinear rotational spring from a linear translational spring. The cable, connected to the linear spring, is wound around a non-circular spool as shown in Fig. 1. The non-circular shape induces a nonlinear relationship between the angular position of the spool and the torque created by the tension of the cable at the spool's axis. Depending on the non-circular shape, various nonlinear torque profiles can be realized. Compared to the mechanisms presented in [15, 16, 19], the cable spool mechanism has the advantage of using very few moving parts. This does not only make the technical realization simpler, but also reduces the erroneous inertial forces that could be applied to the joint by the moving parts [18]. Indeed, the only parts not rigidly connected to the mechanical joint or the spring are the cable and the pulley, which masses are very small. A similar mechanism was

This research is supported by the *Research on Macro/Micro Modeling of Human Behavior in the Swarm and its Control* under the Core Research for Evolutional Science and Technology (CREST) Program (research area: Advanced Integrated Sensing Technologies), Japan Science and Technology Agency (JST).

The authors are with the Department of Mechanical Sciences and Engineering, Tokyo Institute of Technology, 2-12-1 Ookayama, Meguro-ku, 152-8550 Tokyo, Japan schmit.n.aa@m.titech.ac.jp

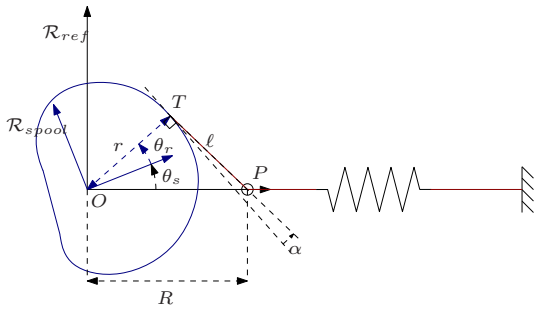

Fig. 1. Transmission mechanism with a non-circular cable spool.

proposed in [22], but the closed-form solution was derived for a different mechanism where the linear spring is replaced by a constant weight.

This paper is organized as follows: section II presents the mechanism, the notations and the list of assumptions. Section III details the methodology to derive the shape of the spool from a prescribed torque profile. We show that this problem has an exact (closed form) solution. Section IV presents the experimental device and the results of experiments carried out on three different shapes of spool. We discuss the possible sources of errors between the theoretical and experimental results.

II. NON-CIRCULAR CABLE SPOOL SYSTEM

We consider the mechanism shown in Fig. 1. A linear spring is connected to a cable which goes through a pulley and is wound around a non-circular spool. The spool axis is rigidly attached to the axis of the mechanical joint (not shown in the figure). $\mathcal{R}_{ref}$ is the reference coordinate frame, $\mathcal{R}_{spool}$ is the coordinate frame attached to the spool, O is the axis of the spool (which is also the origin of $\mathcal{R}_{ref}$ and $\mathcal{R}_{spool}$) and θ_s is the angle of $\mathcal{R}_{spool}$ with respect to $\mathcal{R}_{ref}$. The pulley P is placed on the x axis of $\mathcal{R}_{ref}$ at a distance $R(>0)$ from O. T is the point where the cable is tangent to the spool, $\ell(=TP)$ is the length of cable between the tangency point and the pulley, $r(=OT)$ is the varying radius of the spool, θ_r is the angular position of r with respect to $\mathcal{R}_{spool}$ and α is the angle of the cable at the tangency point with respect to the perpendicular of the varying radius (pressure angle).

Because the spool is not circular, the torque τ generated in O by the tension of the cable is a nonlinear function of the spool's angular position θ_s. The synthesis problem consists in calculating the shape of the spool to synthesize a prescribed torque profile $\tau(\theta_s)$. In the derivation of the equations of the spool's contour, we use the following simplifications:

- The stiffness of the cable is infinite (no stretching)
- The radius of the pulley is null
- The radius of the cable is null[1]

Furthermore, the origin of θ_s is defined such that $0 \leq \theta_s \leq \theta_{s,max}$.

[1]The real radius of the cable is considered *a posteriori* (see section IV).

III. SYNTHESIS OF NON-CIRCULAR SPOOL

A. Geometry of the proposed system

To calculate the shape of the spool, we first translate the prescribed torque profile into a kinematic relationship. From the Principe of Virtual Work:

$$\tau(\theta_s)\, d\theta_s = k\, q\, dq \tag{1}$$

where q is the displacement of the linear spring with respect to its natural length, and k is the spring constant. Since the tension of the cable must be strictly positive, we assume that $\tau(\theta_s) > 0$ and $q > 0$. From (1), we calculate $\frac{dq}{d\theta_s}$ and define the function J as follows:

$$J(\theta_s) = \frac{dq}{d\theta_s} = \frac{\tau(\theta_s)}{\sqrt{2\,k\,\int_0^{\theta_s} \tau(u)\, du + (k\, q_0)^2}} \tag{2}$$

where q_0 is the displacement of the spring when $\theta_s = 0$. $J(\theta_s)$ defines the kinematic input/output relationship that the spool must achieve to synthesize the torque profile $\tau(\theta_s)$. $J(\theta_s)$ can be seen as the translation of a torque synthesis problem into a kinematic synthesis problem.

As shown in Fig. 1, the spool's contour is defined in polar coordinates by the relationship $r(\theta_r)$. Considering that the problem is parameterized by θ_s, we need to determine two independent equations between r, θ_r and θ_s to solve the problem.

B. Tangency condition

We consider the displacement of the tangency point T for a small variation of θ_r, as shown in Fig. 2. We note δa the distance between $T(\theta_r)$ and $T(\theta_r + \delta\theta_r)$. Using the law of cosines, we obtain

$$\begin{aligned}(\delta a)^2 =& (r(\theta_r))^2 + (r(\theta_r + \delta\theta_r))^2 \\ & - 2r(\theta_r)r(\theta_r + \delta\theta_r)\cos(\delta\theta_r)\end{aligned} \tag{3}$$

$$\begin{aligned}(r(\theta_r))^2 =& (r(\theta_r + \delta\theta_r))^2 + (\delta a)^2 \\ & - 2r(\theta_r + \delta\theta_r)\delta a \cos\varphi\end{aligned} \tag{4}$$

We substitute (3) in (4) then calculate the Taylor expansion in $\delta\theta_r$.

$$2r\left(\frac{dr}{d\theta_r} - \sqrt{\left(\frac{dr}{d\theta_r}\right)^2 + r^2}\cos\varphi\right) + \mathcal{O}(\delta\theta_r) = 0 \tag{5}$$

By taking the limit of the above expression when $\delta\theta_r$ tends to 0 then substituting $\lim_{\delta\theta_r \to 0} \varphi$ by $\frac{\pi}{2} + \alpha$, be obtain

$$\tan\alpha = -\frac{1}{r}\frac{dr}{d\theta_r} \tag{6}$$

Equation (6) is called the tangency equation.

C. Conservation of the total length of cable

We note ℓ_{spool} the length of cable wound around the spool, ℓ_{spring} the length of cable from the pulley to the spring and L the total length of cable. Since the total length of cable is constant:

$$\frac{dL}{d\theta_s} = \frac{d\ell_{spool}}{d\theta_s} + \frac{d\ell}{d\theta_s} + \frac{d\ell_{spring}}{d\theta_s} = 0 \tag{7}$$

We now detail the calculation of the three terms of the right hand side of (7).

a) First term:

We calculate the second order Taylor expansion in $\delta\theta_r$ of (3) and remove the term $\frac{dr}{d\theta_r}$ using (6). We obtain

$$(\delta a)^2 = \frac{r^2}{\cos^2\alpha}(\delta\theta_r)^2 + \mathcal{O}\left((\delta\theta_r)^3\right) \tag{8}$$

From (8), we calculate $\frac{d\ell_{spool}}{d\theta_r}$ as follows:

$$\frac{d\ell_{spool}}{d\theta_r} = -\lim_{\delta\theta_r\to 0}\frac{\delta a}{\delta\theta_r} = -\frac{r}{\cos\alpha} \tag{9}$$

Thus, the first term of the right hand side of (7) is

$$\frac{d\ell_{spool}}{d\theta_s} = -\frac{r}{\cos\alpha}\frac{d\theta_r}{d\theta_s} \tag{10}$$

b) Second term:

Using the law of cosines in Fig. 1, ℓ is calculated as follows:

$$\ell = \sqrt{R^2 + r^2 - 2\,R\,r\,\cos(\theta_r+\theta_s)} \tag{11}$$

The total derivative of ℓ with respect to θ_s is represented by:

$$\frac{d\ell}{d\theta_s} = \left(\frac{\partial l}{\partial\theta_r} + \frac{\partial l}{\partial r}\frac{dr}{d\theta_r}\right)\frac{d\theta_r}{d\theta_s} + \frac{\partial\ell}{\partial\theta_s} \tag{12}$$

We use (11) to calculate the partial derivatives of ℓ and (6) to remove the term $\frac{dr}{d\theta_r}$. We obtain

$$\frac{d\ell}{d\theta_s} = \frac{r}{\cos\alpha}\frac{d\theta_r}{d\theta_s} + \frac{R\,r}{\ell}\sin(\theta_r+\theta_s) \tag{13}$$

c) Third term:

Since the pulley and the anchor of the spring are fixed, the length $\ell_{spring} + q$ is constant. Thus, we obtain from (2)

$$\frac{d\ell_{spring}}{d\theta_s} = -\frac{dq}{d\theta_s} = -J(\theta_s) \tag{14}$$

An important point is that *we do not impose the angle α to be small*. $\delta\theta_r$ is an abstract variable used to derive the tangency condition but has no physical meaning in the real mechanism. Since (6) and (9) are *by definition* the limit of (5) and (8) when $\delta\theta_r$ tends to zero, the solution derived is exact.

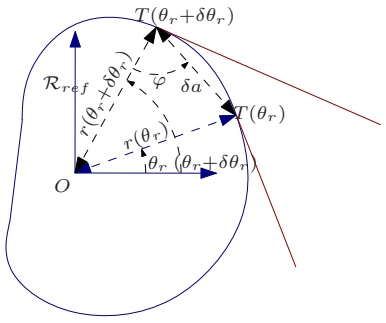

Fig. 2. Displacement of tangency point

D. Calculation of explicit solution

By substituting (10), (13) and (14) in (7), we obtain the following equation:

$$\frac{R\,r}{\ell}\sin(\theta_r+\theta_s) = J(\theta_s) \tag{15}$$

This is a first constraint relationship between r, θ_r and θ_s. We now substitute (11) in (15), take the square of this equation, and write it as

$$\mathcal{G} = \frac{R^2\,r^2\,\sin^2(\theta_r+\theta_s)}{R^2+r^2-2\,R\,r\,\cos(\theta_r+\theta_s)} = J^2(\theta_s) \tag{16}$$

Using (6) to remove the term $\frac{dr}{d\theta_r}$, the derivative of this equation with respect to θ_s is

$$\frac{d\mathcal{G}}{d\theta_s} = \left(\frac{\partial\mathcal{G}}{\partial\theta_r} - r\,\tan\alpha\,\frac{\partial\mathcal{G}}{\partial r}\right)\frac{d\theta_r}{d\theta_s} + \frac{\partial\mathcal{G}}{\partial\theta_s} = 2\,J(\theta_s)\,J'(\theta_s) \tag{17}$$

Where $J'(\theta_s)$ stands for $\frac{dJ(\theta_s)}{d\theta_s}$.

Equation (17) should lead to a differential equation on $\frac{d\theta_r}{d\theta_s}$. However, the value of $(\frac{\partial\mathcal{G}}{\partial\theta_r} - r\,\tan\alpha\,\frac{\partial\mathcal{G}}{\partial r})$ is exactly zero no matter the values of r, θ_r, and θ_s. Thus, (17) is reduced to:

$$\frac{d\mathcal{G}}{d\theta_s} = \frac{\partial\mathcal{G}}{\partial\theta_s} = 2\,J(\theta_s)\,J'(\theta_s) \tag{18}$$

Using (16) to calculate $\frac{\partial\mathcal{G}}{\partial\theta_s}$, we obtain

$$\begin{aligned}&\frac{R^2\,r^2}{\ell^4}\sin(\theta_r+\theta_s)\\ &\cdot\left[\cos(\theta_r+\theta_s)\,(R^2+r^2) - (1+\cos^2(\theta_r+\theta_s))\,R\,r\right]\\ &= J(\theta_s)\,J'(\theta_s)\end{aligned} \tag{19}$$

This is a second constraint relationship between r, θ_r and θ_s. For a given set of θ_s, the spool contour is defined by the set of (r,θ_r) solution of the system (15),(19).

We now solve the system (15),(19) to obtain the explicit solution of the spool contour. After substituting ℓ using (11), equation (15) is equivalent to

$$R^2r^2X^2 - 2RrJ^2X + (R^2+r^2)J^2 - R^2r^2 = 0 \tag{20}$$

where $X = \cos(\theta_r+\theta_s)$. Note that to clarify the equations, we use the simplified notation J instead of $J(\theta_s)$. Assuming that $0 < J \le r < R$, the roots of (20) are

$$\begin{aligned}X &= \frac{RrJ^2 \pm \sqrt{\Delta}}{R^2r^2}\\ \Delta &= R^2r^2\,(R^2-J^2)\,(r^2-J^2)\end{aligned} \tag{21}$$

Thus, θ_r is obtained as:

$$\theta_r = -\theta_s + \arccos\left(\frac{J^2 \pm \sqrt{(r^2-J^2)\,(R^2-J^2)}}{R\,r}\right) \tag{22}$$

The $\pm$ symbol in (22) comes from the two distinct roots of (20). We will show later that this symbol must be chosen equal to $\mathrm{sgn}(J')$.

After substituting (11) and (22), (19) is equivalent to

$$\frac{R^2\, r^2 \sqrt{1-\left(\frac{1}{R\,r}\,\left(J^2 \pm \Lambda\right)\right)^2}}{\left(R^2+r^2-2\,R\,r\,\left(\frac{1}{R\,r}\,\left(J^2 \pm \Lambda\right)\right)\right)^2} \left(r\left(\frac{1}{R\,r}\,\left(J^2 \pm \Lambda\right)\right)-R\right) \cdot\left(r-R\left(\frac{1}{R\,r}\,\left(J^2 \pm \Lambda\right)\right)\right) = J\,J' \qquad (23)$$

where $\Lambda = \sqrt{(r^2-J^2)\,(R^2-J^2)}$. We now define $r^* = \sqrt{r^2-J^2}$ and $R^* = \sqrt{R^2-J^2}$. Equation (23) is equivalent to

$$\pm\frac{r^*R^*}{R^* \mp r^*} = J' \qquad (24)$$

Since we imposed the condition $r < R$, $(R^* \mp r^*)$ is positive. Thus, the $\pm$ symbol in (22), (23) and (24) must be chosen equal to $\mathrm{sgn}(J')$. From (24), the explicit solution of r is obtained as:

$$r = \sqrt{J^2(\theta_s) + \frac{J'^2(\theta_s)\,(R^2-J^2(\theta_s))}{\left(J'(\theta_s)+\sqrt{R^2-J^2(\theta_s)}\right)^2}} \qquad (25)$$

We note that this last equation does not depend on $\mathrm{sgn}(J')$. The system (22),(25) defines the unique explicit solution of the spool contour for a given function $J(\theta_s)$. For a given set of θ_s, we first use (2) to calculate J, then we use (25) to calculate the set of r and finally we use (22) to calculate the set of θ_r. An important remark is that a necessary condition so that a solution exists is $J \leq r$. Under this condition, the radius of the spool verifies the relationship $J(\theta_s) \leq r(\theta_s) < R$. Furthermore, since the tension in the cable must stay positive, the objective torque profile $\tau(\theta_s)$ must be strictly positive.

E. Example of design

To illustrate the design methodology, we calculated three different spools realizing a constant force spring, an exponential softening spring and a cubic polynomial spring. The shape of the spools is shown in Fig. 3(a), Fig. 4(a) and Fig. 5(a), the prescribed torque profile is shown in Fig. 3(b), Fig. 4(b) and Fig. 5(b), the varying radius r is shown in Fig. 3(c), Fig. 4(c) and Fig. 5(c) and the torsional stiffness of the mechanism is shown in Fig. 3(d), Fig. 4(d) and Fig. 5(d). The spools are shown at the angular position $\theta_s = 0$, and rotate counterclockwise when θ_s increases. G is the center of mass. The angular displacement range is $[0°, 270°]$ (identical for the three spools). As shown in Fig. 5, although the spring is always pulled when the spool rotates counterclockwise, it is possible to realize a torque profile with a locally negative stiffness. This is achieved by a sudden drop in the radius r.

F. Choice of design parameters

In the derivation of the equations of the spool (J (2), r (25), θ_r (22)), we introduced three design parameters: the spring constant k, the spring preloading $(k\,q_0)$ and the location of the pulley R. Since the prescribed torque profile

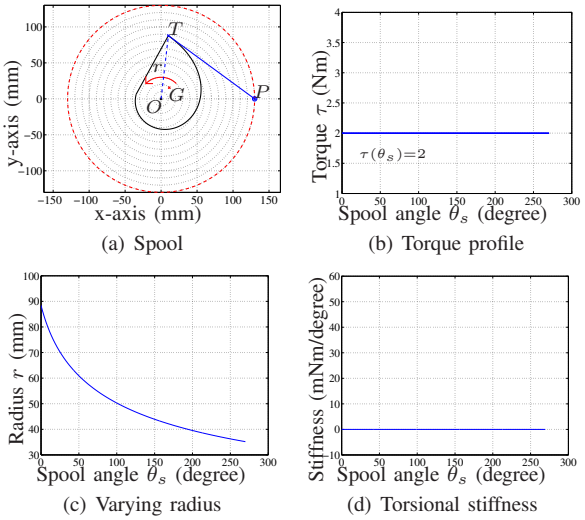

(a) Spool (b) Torque profile (c) Varying radius (d) Torsional stiffness

Fig. 3. Constant force spring

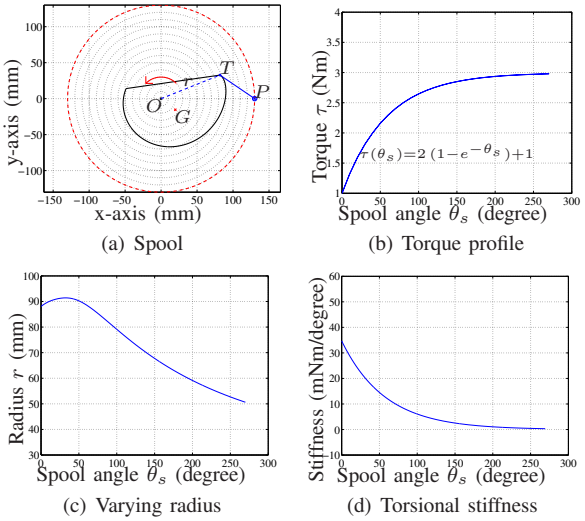

(a) Spool (b) Torque profile (c) Varying radius (d) Torsional stiffness

Fig. 4. Exponential softening spring

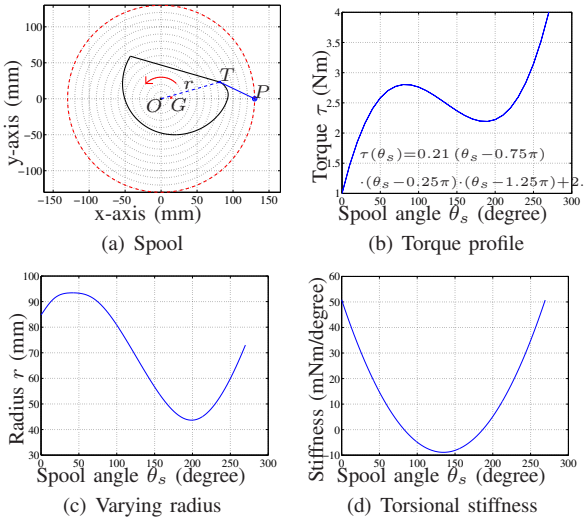

(a) Spool (b) Torque profile (c) Varying radius (d) Torsional stiffness

Fig. 5. Cubic polynomial spring

is embedded in (2), a change of one or several design parameters results in a different spool shape but does not affect the torque profile of the mechanism. We illustrate this property with a simple example: for each set of design parameters shown in Table I, we calculated the spool synthesizing the torque profile shown in Fig. 5(b). The spools are shown in Fig. 6.

The set $\{k, q_0, R\}$ can be chosen to optimize a design criterion, such as minimizing the size of the mechanism. However, calculating the set $\{k, q_0, R\}$ which optimizes a given design criterion is a complicated optimization problem because the equations of the spool are highly nonlinear, and because the design has to satisfy complicated geometric constraints to ensure that the contour is convex and without loops. In this paper, we will not say further about the optimization of the design parameters as it will addressed in a future publication.

IV. EXPERIMENTS

A. Description of the experimental device

The experimental device is shown in Fig. 7. From the right to the left: the spool, a torque sensor, a harmonic gear, and a handle. Thanks to the high reduction ratio of the harmonic gear (1:50), the spool can be rotated easily by the experimentator using the handle. We use a scale printed on the handle to measure the position of the spool. In this experiment, we neglect the angular error due to the twist of the kinematic chain (gear+couplings+sensor).

TABLE I

DESIGN PARAMETERS

k (N/m)	q_0 (mm)	R (mm)
137	130	130
170	140	100
205	170	70
1233	127	24

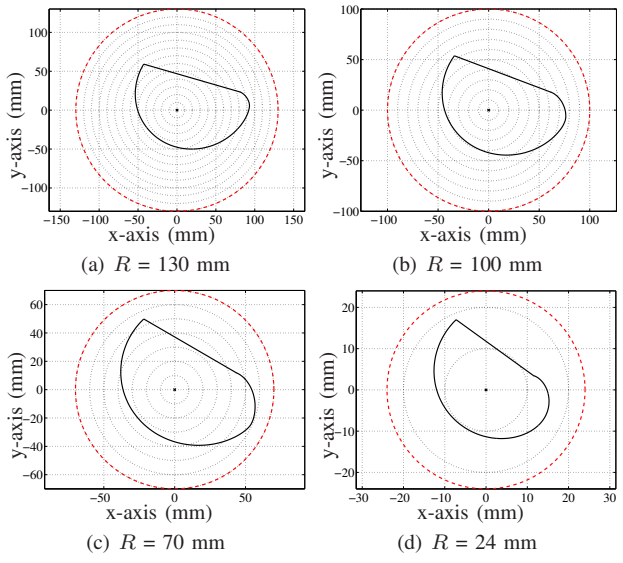

(a) R = 130 mm (b) R = 100 mm

(c) R = 70 mm (d) R = 24 mm

Fig. 6. Spools calculated with the same torque profile but different design parameters

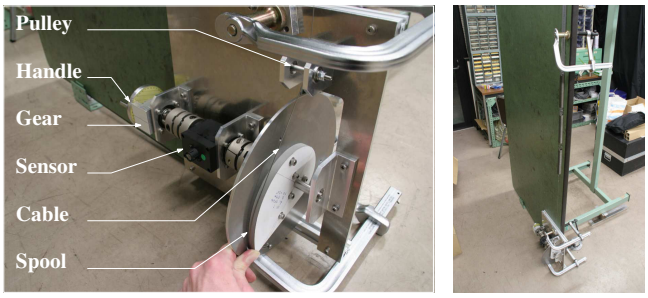

Fig. 7. Experimental device

Indeed, the torsional stiffness of the kinematic chain from the handle to the spool is 313 Nm/rad and since in our experiments the torque at the spool's axis does not exceed 4 Nm, the maximum angular error is 0.732°. The experiments are carried out with the 3 spools presented in section III-E. The spools are cut in an 8 mm thick aluminum board using a wire-cut machine tool. The spool masses are 172 g, 226 g and 233 g respectively. In order to take into account the thickness of the wire, we removed 0.4 mm from the theoretical radius r. The cable is a steel wire which diameter is 0.8 mm. We assume the stretching of the cable to be negligible. The linear spring, which consists in 3 identical springs in series, has a stiffness constant of 137 N/m. The pulley has a diameter of 6 mm and is located 130 mm from the axis of the spool.

B. Results of experiments

The comparison of the theoretical (blue solid line) and experimental (black x-mark line) torque profile is shown in Fig. 8(a), 9(a) and 10(a). The experiments consisted in increasing θ_s from 0°to 270°, then decreasing θ_s back to 0°. We subtracted from the experimental data the gravity moment due to the weight of the spool (calculated as a function of θ_s using the mass and location of the center of mass). The relative torque error is shown in Fig. 8(b), 9(b) and 10(b). The average torque error for the three spools is about 1.5%. The error consists mainly in a hysteresis effect (higher torque when increasing θ_s) which might be caused by friction in the ball bearings. This can be easily seen in Fig. 10(b). However, in Fig. 9(b) the error seems to be correlated with the position of the spool. A possible explanation is a small error in the preloading $(k\, q_0)$, which affects the load-displacement function. In future designs, we plan to add a screw to finely tune the preloading in order to increase the accuracy of the synthesized torque profile.

V. CONCLUSIONS

In this paper, we proposed a cable mechanism based on a non-circular spool which synthesizes a nonlinear rotational spring from a linear spring. We showed that for a prescribed torque profile $\tau(\theta_s)$, there is a closed-form solution of the shape of the spool which synthesizes this function. We derived the equations of the spool, then verified the design methodology by experiments with three different spools realizing a constant force spring, an exponential softening spring and a cubic polynomial spring. The experiments

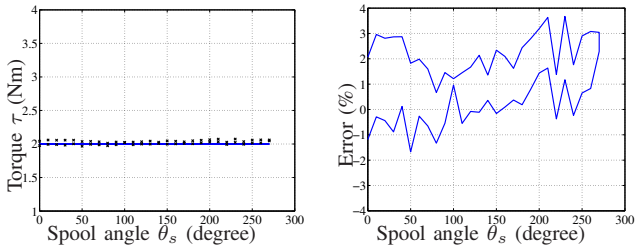

(a) Torque vs. spool's angular position (b) Relative torque error

Fig. 8. Constant force spring

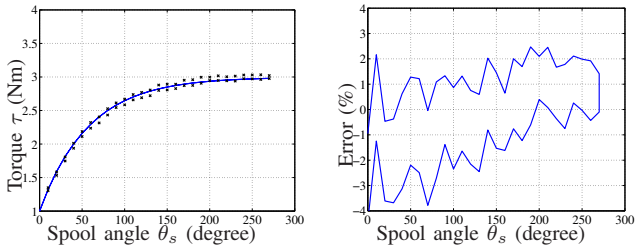

(a) Torque vs. spool's angular position (b) Relative torque error

Fig. 9. Exponential softening spring

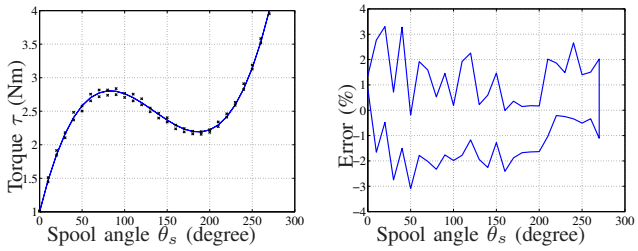

(a) Torque vs. spool's angular position (b) Relative torque error

Fig. 10. Cubic polynomial spring

showed that the prescribed torque profiles where achieved with an average accuracy of 1.5%. This mechanism has the advantage of using very few moving parts, which makes it easy to manufacture and reduces the erroneous inertial forces that could be applied to the joint by moving parts. Furthermore, the size of the spool can be scaled by changing the design parameters k, q_0 and R.

Future work will include the development of a compact nonlinear spring unit which could fit in the ankle joint of a walking robot. We also plain to develop an antagonistic mechanism which could synthesize a torque profile with both positive and negative magnitude. Further studies will address the conditions that a torque profile must satisfy to be realizable with this mechanism.

REFERENCES

[1] E. Suhir. "Shock protection with a nonlinear spring". In: *IEEE Transactions on Components, Packaging, and Manufacturing Technology* 18.2 (June 1995), pp. 430–437.

[2] Jung-Jun Park, Byeong-Sang Kim, Jae-Bok Song, and Hong-Seok Kim. "Safe Link Mechanism based on Passive Compliance for Safe Human-Robot Collision". In: *Proc. IEEE International Conference on Robotics and Automation*. Roma, Italy, Apr. 2007, pp. 1152–1157.

[3] Jung-Jun Park, Hwi-Su Kim, and Jae-Bok Song. "Safe robot arm with safe joint mechanism using nonlinear spring system for collision safety". In: *Proc. IEEE International Conference on Robotics and Automation*. Kobe, Japan, May 2009, pp. 3371–3376.

[4] Xiaoai Jiang, D. Michael McFarland, Lawrence A. Bergman, and Alexander F. Vakakis. "Steady State Passive Nonlinear Energy Pumping in Coupled Oscillators: Theoretical and Experimental Results". In: *Nonlinear Dynamics*. Vol. 33. 1. Springer Netherlands, July 2003, pp. 87–102.

[5] D. Michael McFarland, Lawrence A. Bergman, and Alexander F. Vakakis. "Experimental study of non-linear energy pumping occurring at a single fast frequency". In: *International Journal of Non-Linear Mechanics* 40.6 (2005), pp. 891–899.

[6] R. McN. Alexander. "Three uses for springs in legged locomotion". In: *International Journal of Robotics Research* 9.2 (Apr. 1990), pp. 53–61.

[7] J. Yamaguchi and A. Takanishi. "Design of biped walking robots having antagonistic driven joints using nonlinear spring mechanism". In: *Proc. IEEE/RSJ International Conference on Intelligent Robots and Systems*. Vol. 1. Grenoble, France, Sept. 1997, pp. 251–259.

[8] D. Owaki and A. Ishiguro. "Enhancing Stability of a Passive Dynamic Running Biped by Exploiting a Nonlinear Spring". In: *Proc. IEEE/RSJ International Conference on Intelligent Robots and Systems*. Beijing, China, Oct. 2006, pp. 4923–4928.

[9] Katja D. Mombaur, Richard W. Longman, Hans Georg Bock, and Johannes P. Schloder. "Open-loop stable running". In: *Robotica* 23.01 (2005), pp. 21–33. eprint: `http://journals.cambridge.org/article_S026357470400058X`.

[10] V. E. Berbyuk and A. E. Bostrom. "Optimization Problems of Controlled Multibody Systems Having Spring-Damper Actuators". In: *International Applied Mechanics* 37 (7 2001), pp. 935–940.

[11] Christine Vehar Jutte. "Generalized Synthesis Methodology Of Nonlinear Springs For Prescribed Load-Displacement Functions". PhD thesis. University of Michigan, 2008.

[12] Christine Vehar Jutte and Sridhar Kota. "Design of Single, Multiple, and Scaled Nonlinear Springs for Prescribed Nonlinear Responses". In: *Journal of Mechanical Design* 132.1 (2010), p. 011003.

[13] Christine Vehar Jutte and Sridhar Kota. "Design of Nonlinear Springs for Prescribed Load-Displacement Functions". In: *Journal of Mechanical Design* 130.8 (2008), p. 081403.

[14] Chad English and Donald Russell. "Implementation of variable joint stiffness through antagonistic actuation using rolamite springs". In: *Mechanism and Machine Theory* 34.1 (1999), pp. 27–40.

[15] M. Okada and J. Takeishi. "Kineto-static mechanical synthesis for nonlinear property design of passive stiffness using closed kinematic chain". In: *Proc. IEEE/RSJ International Conference on Intelligent Robots and Systems*. Taipei, Taiwan, Oct. 2010, pp. 4213–4218.

[16] S.A. Migliore, E.A. Brown, and S.P. DeWeerth. "Biologically Inspired Joint Stiffness Control". In: *Proc. IEEE International Conference on Robotics and Automation*. Barcelona, Spain, Apr. 2005, pp. 4508–4513.

[17] S. Wolf and G. Hirzinger. "A new variable stiffness design: Matching requirements of the next robot generation". In: *Proc. IEEE International Conference on Robotics and Automation*. Pasadena, CA, USA, May 2008, pp. 1741–1746.

[18] Shane A. Migliore, Edgar A. Brown, and Stephen P. DeWeerth. "Novel Nonlinear Elastic Actuators for Passively Controlling Robotic Joint Compliance". In: *Journal of Mechanical Design* 129.4 (2007), pp. 406–412.

[19] Jonathan W. Hurst, Joel Chestnutt, and Alfred Rizzi. *An Actuator with Mechanically Adjustable Series Compliance*. Tech. rep. CMU-RI-TR-04-24. Pittsburgh, PA, USA: Robotics Institute, Carnegie Mellon University, Apr. 2004.

[20] K. Koganezawa. "Mechanical stiffness control for antagonistically driven joints". In: *Proc. IEEE/RSJ International Conference on Intelligent Robots and Systems*. Edmonton, Alberta, Canada, Aug. 2005, pp. 1544–1551.

[21] Takashi Sonoda, Yuya Nishida, and Kazuo Ishii. "Adaptable Compliance and Motion Control Employing Kinematic Transmission Mechanisms (in Japanese)". In: *Proc. The 28th Annual Conference of the Robotics Society of Japan*. RSJ2010AC3O2-5. Nagoya, Japan, Sept. 2010.

[22] P. H. Tidwell, N. Bandukwala, S. G. Dhande, C. F. Reinholtz, and G. Webb. "Synthesis of Wrapping Cams". In: *Journal of Mechanical Design* 116.2 (June 1994), pp. 634–638.